Optimization of Machining Parameters in Turning for Different Hardness using Multi-Objective Genetic Algorithm

Mimi Muzlina Mukri, Nor Atiqah Zolpakar[*]
Faculty of Mechanical and Automotive Engineering Technology,
Universiti Malaysia Pahang, 25200 Pekan, Pahang, MALAYSIA
[*]*noratiqahz@ump.edu.my*

Sunil Pathak
HiLASE Center, Institute of Physics, Czech Academy of Sciences,
Za Radnici 828, 25241 Dolni Brezany, CZECH REPUBLIC

ABSTRACT

Surface finish and temperature rise are the crucial machining outcomes since it determines the quality of the machining and the tool life. During machining operations, choosing optimal machining parameters is critical since it affects the machining outcome. In this work, Multi-Objective Genetic Algorithm (MOGA) optimization is used to find the combination of machining parameters at different levels of hardness of 20, 36, and 43 to obtain minimum surface roughness and minimum cutting temperature in turning operation. Cutting depth, cutting speed, and feed rate are the machining variables that are used in the process of optimization. From the results, it shows that the minimum temperature rise is 243.333 ℃ with a surface roughness of 1.975 µm during machining of 20 hardness. It also observed that the hardness of the material significantly affects the surface roughness and temperature rise. The outcome shows that as the hardness of the material is increasing the temperature is increasing while the surface roughness is decreasing. This research also revealed that using a MOGA to optimize multi-objective replies produces positive outcomes.

Keywords: *Optimization; Machining Parameters; Genetic Algorithm; Turning*

ISSN 1823-5514, eISSN 2550-164X
© 2023 College of Engineering,
Universiti Teknologi MARA (UiTM), Malaysia
https://doi.org/10.24191/jmeche.v20i3.23899

Received for review: 2022-06-01
Accepted for publication: 2023-05-09
Published: 2023-09-15

Introduction

Turning is the process of eliminating metal from the external diameter of a revolving cylindrical workpiece by lowering the workpiece's diameter to a predetermined size while achieving a smooth metal surface [1]. This machining method is one of the most critical in creating components for a wide range of applications, including prototypes like custom-designed shafts and fasteners that are utilised in small quantities [2]. It is critical to choose cutting parameters for turning operations in order to obtain excellent cutting performance [3]. During machining, the cutting zone temperature is extremely high, and the chip absorbs the majority of the heat generated by the cutting operation. Tool wear, tool life, and surface quality all suffer as a result of high temperatures [4]-[5]. This statement is supported by Pimenov et al. [6] recent study is focused on cutting tool wear, cutting force determination, surface roughness fluctuations, and other machining reactions. Variations in these machining reactions cause significant changes in dimensional accuracy and productivity [7]. For every machining operation, high cutting temperatures and their associated detrimental consequences are a major problem. This must be controlled in order to enhance machined product quality, reduce machining costs, and increase production rates [8]. According to Halim et al. [9], excessive heat would develop in the cutting zone, raising the cutting temperature. As a result of this circumstance, cutting force and tool wear rates increased rapidly, and the surface quality deteriorated [9]. So, the optimization of this process is required to improve the efficiency of the process.

As stated by Bhuiyan et al. [10], many academics have been focused on optimizing process parameters in machining by devising an analytical technique for determining the ideal cutting speed in a single stage turning process since 1950. Generally, optimization methods can be classified into two which are conventional methods and non-conventional methods. Traditional approaches such as ANOVA, the Taguchi method, and others start with an estimation and converge towards the optimal solution with each iteration. This convergence is determined by the starting approximation used. Although traditional approaches are claimed to be effective in addressing one type of machining optimization issue, they may not be effective in tackling another [11]. There are still a few researchers using this technique in their studies. The Taguchi method was used by Akkus and Yakka [12] to determine the best value of surface roughness and the most effective parameters that contribute to surface roughness. According to the findings, among the three factors involved, cutting speed, feed rate, and cutting depth, the feed rate is the most important element that leads to surface roughness [12]. Using the Taguchi and ANOVA methodologies, Krishna et al. [13] and Palaniappan et al. [14] conducted research that highlighted the optimisation of turning process parameters to achieve excellent surface

quality. According to the findings, both researchers agree, the feed rate is the significant parameter that will affect surface roughness.

In recent years, engineering optimization problems have seen an increase in popularity for non-traditional optimization techniques including Genetic Algorithms (GA), Simulated Annealing (SA), Artificial Neural Networks (ANN), and many more approaches. These algorithms have been discovered to be promising search and optimization techniques for complicated optimization issues. The same approach hired by Shah et al. [15], Manav and Chinchanikar [16], Durga et al. [17], and Narayan et al. [18] which is a multi-objective genetic algorithm (MOGA), to optimize machining settings such as that response variables including cutting force, temperature, material removal rate and surface roughness were optimized to their ideal range. The factors that affect each response variable are cutting speed, feed rate, and depth of cut.

To observe the effectiveness of conventional with non-conventional optimization, a lot of researchers mixed conventional and non-conventional methods in their study to optimize the machining parameters in turning operations. Kumar et al. [19] and Butola et al. [20] used the same Taguchi, ANOVA, and GA methodologies to optimize machining settings in order to get the finest Material Removal Rate (MRR), surface roughness, and temperature values. Taguchi and ANOVA are utilized to discover key values. ANOVA and GA are used to optimize process parameters and are agreed upon by both researchers. Mia and Dhar [21] provide work on the development of mathematical by using Response Surface Methodology (RSM), fuzzy inference system (FIS) to formulate the predictive model and simulated annealing (SA) in order to formulate the optimization model for the average surface roughness parameter in turning. The model is solved using GA, and the ideal start time for non-critical processes as well as the ideal duration for each process are determined [22]. Chabbi et al. [23] investigated the influence of cutting parameters on surface roughness, cutting force, cutting power, and productivity during turning using three optimisation techniques: RSM, Artificial Neural Network (ANN), and Desirability Function (DC). Bolivar et al. [24] employed an ANN and a GA to create a system that optimizes cutting insert selection and cutting parameters throughout the turning process (GA). This previous research showed that GA has a good reputation in searching optimize solutions not just single objective but multi-objective problems [7].

According to the background literature, a substantial study has been done on the relationship between the turning process and surface roughness. However, there have only been a few attempts to optimise the temperature rise during the turning process, despite the fact that this is one of the crucial factors that can affect both the surface roughness and tool life. The purpose of this study is to determine how cutting speed, feed rate, and depth of cut affect temperature increase and surface roughness when the material

hardness has been changed, given the relevance of temperature rise and surface roughness in the turning process.

Optimization using Multi-Objective Genetic Algorithm (MOGA)

For parametric optimization, the genetic algorithm has proved to be one of the most common multi-objective optimization strategies. Given that it works with a population of potential solutions, a genetic algorithm can be used to solve multi-objective optimisation problems and find many solutions simultaneously [25]. This function was used as the objective function in the MOGA Toolbox of MATLAB 2018b. For the optimization of surface roughness and the minimizing of temperature rise in turning, the objective function values are determined accordingly.

In this study, the optimization was conducted to obtain minimum temperature rise and also smaller surface roughness during the turning process. To generate minimum surface roughness, the machining setup needs to be set to high speed, and this will course a temperature rise at the tool and also the workpiece. Because these two goals are incompatible, MOGA optimization is utilized to discover the feed rate, depth of cut, and cutting speed combination that creates the best surface roughness and temperature rise throughout the machining process. The objective functions for this work can be represented as follow:

$$f_1 = Min\, T\,(f, d, v)$$

$$f_2 = Min\, Ra\,(f, d, v)$$

The objective function used to represent temperature rise and surface roughness for the turning process is based on work by Tanikic [26] using RSM modelling. Equations (1) and (2) represent the objective function for temperature rise and surface roughness that has been used in this optimization [26].

$$T = -96.769 + 6.665.HRC + 1.659.V + 247.165.f + 113.067.a \quad (1)$$

$$Ra = 4.365 - 0.0501.HRC - 0.0156.V + 9.007.f + 0.225.a \quad (2)$$

While HRC is the hardness of materials, V is cutting speed, f is feed rate and a is depth of cut.

The algorithm is initiated by generating a randomly initial population. The initial population is made up of several factors that must be optimized, such as depth of cut, cutting speed, and feed rate in this example. The random number was chosen based on the lower and upper limits for each variable. The workpiece material was steel, AISI designation 4140, with dimensions 45 x 250 m. The cutting tool used and assembled of two parts is adopted: cutting tool holder PCLNR 32 25 P12, cutting tool insert CNMG 12 04 08 (grade 235). The lower and upper bounds for the variable parameters are listed below:

$80 \leq$ cutting speed, $v \leq 140$

$0.071 \leq$ feed rate, $f \leq 0.321$

$0.5 \leq$ depth of cut, $a \leq 2.0$

These values were chosen based on the common setup used in the turning operation as reported by [25]. After a randomly initial population was created, then the real numbers of parameters transform into a sequence of a number of binary codes that know as a string. The string consists of chromosomes that indicate possible solutions. The independent variables are coded by a set of genes on the chromosome. The number of bits in the string equals the length of the chromosome, *L*. Each answer is offered by the *L*-bit binary code of chromosome, *C*. There are 2^L -1 viable solutions for choosing. The optimization process began with the creation of a chromosome containing the parameters that needed to be tweaked. The following is a generic representation:

$$C_k = [X_{k1}, X_{k2 \ldots} X_{kn}]$$

$$C_k = [|110 \ldots 00|\underbrace{|101 \ldots 1|}_{X_1}\underbrace{|001 \ldots 11|}_{X_2}\underbrace{|]}_{X_3}$$

where X_1, X_2, and X_3 are the depth of cut, cutting speed, and feed rate respectively. The first generation of the population is then formed, complete with fitness function values. The next stage is to assess each chromosome in the population to see how it will be used in the second generation. There are numerous techniques for selecting chromosomes to be passed down to the next generation, but the operator utilized in this work is a tournament.

The tournament selection technique is carried out by putting selection pressure on the participants by holding a tournament with *s* contestants. In a tournament, for example, there are *s*=6 competitors. Six solutions will compete in a tournament, with the winner advancing to the mating pool. As demonstrated in Figure 1, each solution managed to participate in precisely two tournaments since the event was run in a methodical manner. The number of populations in the selection operator remains the same, but the new population has two better copies. The tournament winner, who has

greater average fitness than the general population, is included in the mating pool.

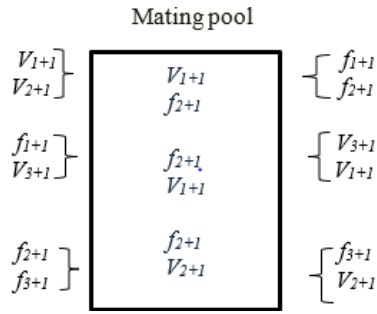

Figure 1: Tournament selection process with 6 contestants

The chromosome will go through a crossover phase after the selection operator. Since the reproduction phase would either replicate a good solution or eradicate the poor solution, no new solution is formed in the population during this phase. The crossover and mutation operators are used to generate a new solution. To create a new solution or offspring, the crossover operator selects two solutions (parents) from the mating pool and switches certain string segments between the two solutions at random positions on the string.

One drawback of the crossover operator is that not all of the newly produced children are better than their parents. Regardless of whether the new offspring is better or worse, other cross-sites or two other strings are picked for the crossing. While the offspring product of the crossover may not create better results than either parent solution, it is apparent that the probability of creating better solutions is higher than with random selection. This is due to reproduction, the operator before the crossing, being active. The representations of the string are probably going to have some advantageous bit combinations if the solution makes it through the tournament reproduction phase. Despite the fact that the crossover produces a poor solution, the bad solutions are removed during the subsequent reproduction step, leading to the conclusion that bad solutions have a brief life cycle. There is a chance you will receive a horrible solution, but there is also a chance you will get a good one. Because the offspring outperforms their parents, more reproductions are predicted in successive reproduction operations, and these solutions are more likely to survive until the following generation's crossover operator. As a result, as the number of iterations increases, so does the number of solutions in the population with comparable chromosomes.

The algorithm will next go on to the mutation operator, which alters a string locally in order to build a better string. For each bit, the bit-wise

mutation process needs the creation of a random integer. The solution in the population is then evaluated to decide whether to stop the algorithm or generate a new generation. This procedure is continual until the termination condition is reached. The flowchart of MOGA can be summarized in Figure 2. The operator setup that is used in the MOGA is listed in Table 1.

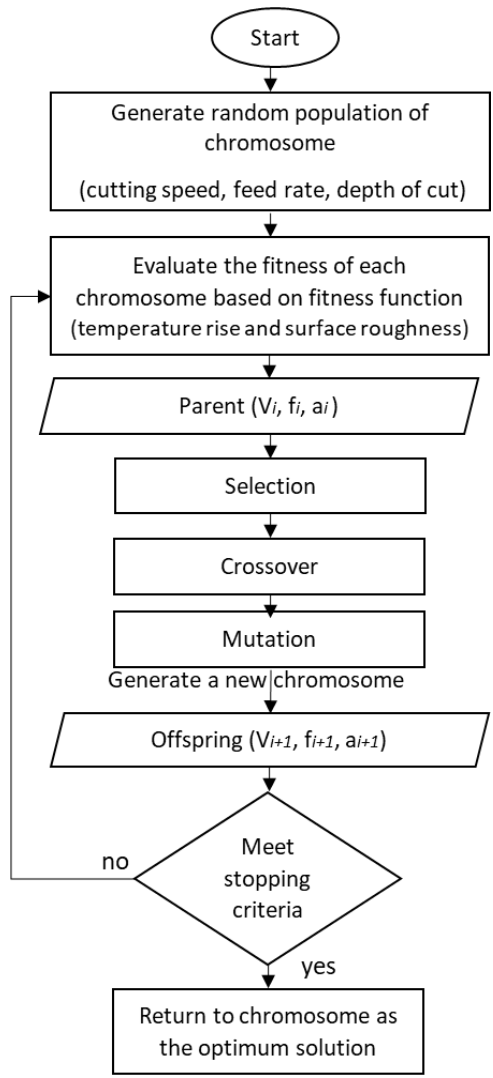

Figure 2: A flowchart of working principle of genetic algorithm

Table 1: Operators for MOGA

Parameters	Setting values
Population size, *N*	50
Generation	300
Selection function	Tournament
Crossover probability, *Pc*	0.8
Crossover function	Intermediate
Mutation function	Constraint dependent

Results and Discussion

Figures 3, 4, and 5 show the Pareto-optimal solutions for various hardness. The Pareto front for temperature increase and surface roughness for hardness 20 HRC is shown in Figure 3. Based on Figure 3, the Pareto front consists of 18 pareto-optimal solutions, and the algorithm converged at 140 generations. When the cutting parameters are 80 m/min, 0.071 mm/rev, and 0.5 mm for cutting speed, feed rate, and depth of cut, the lowest temperature rise achievable in this method is 243.333 °C. Meanwhile, the smallest surface roughness observed is 1.975 µm. The other solutions obtained in the Pareto front are listed in Table 2.

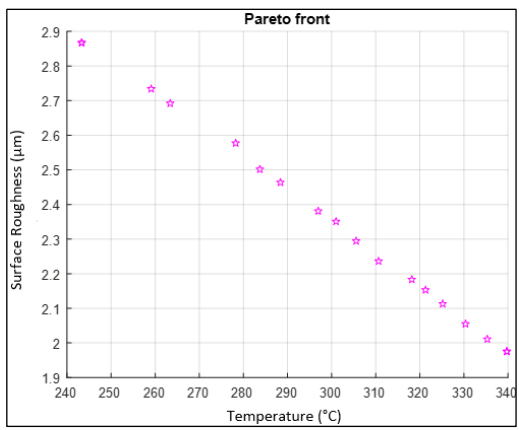

Figure 3: Pareto optimal front for hardness 20 HRC

Figure 4 shows the Pareto front for the temperature and surface roughness for the hardness 36 HRC. The Pareto front has 18 Pareto-optimal solutions, according to Figure 4, and the algorithm converged at generation 506. The lowest temperature rise achieved in this method is 363.071 °C when

the cutting parameters are 85.023 m/min, 0.084 mm/rev, and 0.504 mm for cutting speed, feed rate, and depth of cut, respectively. In the meanwhile, the least surface roughness found is 1.246 µm. Table 3 lists the alternative Pareto front solutions.

Table 2: Pareto optimal solutions for hardness 20 HRC

No	Cutting speed (m/min)	Feed rate (mm/rev)	Depth of cut (mm)	Temperature (°C)	Surface roughness (µm)
1	80.000	0.071	0.500	243.333	2.867
2	137.579	0.072	0.506	339.731	1.975
3	135.026	0.071	0.506	335.284	2.011
4	137.579	0.072	0.506	339.731	1.975
5	132.284	0.071	0.502	330.356	2.055
6	99.853	0.073	0.513	278.244	2.577
7	128.646	0.071	0.509	325.175	2.113
8	80.000	0.071	0.500	243.333	2.867
9	114.039	0.072	0.507	301.002	2.351
10	106.522	0.072	0.507	288.388	2.463
11	126.224	0.072	0.510	321.286	2.153
12	124.417	0.072	0.509	318.181	2.183
13	120.469	0.071	0.502	310.647	2.236
14	103.947	0.072	0.504	283.728	2.501
15	117.226	0.072	0.502	305.565	2.294
16	91.631	0.072	0.505	263.391	2.692
17	111.625	0.072	0.509	296.957	2.381
18	89.028	0.072	0.505	259.079	2.734

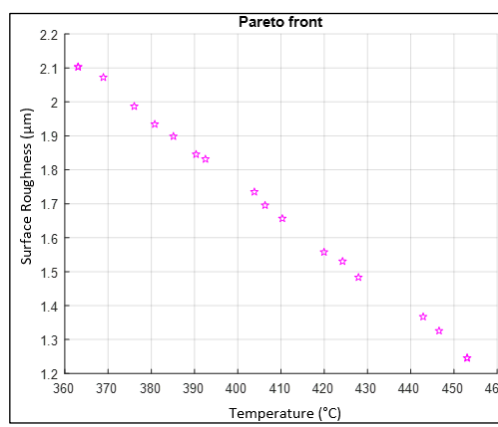

Figure 4: Pareto optimal front for hardness 36 HRC

Table 3: Pareto optimal solutions for hardness 36 HRC

No	Cutting speed (mm/min)	Feed rate (mm/rev)	Depth of cut (mm)	Temperature (°C)	Surface roughness (µm)
1	139.969	0.084	0.504	453.044	1.246
2	85.203	0.084	0.511	363.071	2.103
3	85.203	0.084	0.511	363.071	2.103
4	139.969	0.084	0.504	453.044	1.246
5	121.978	0.084	0.512	424.234	1.530
6	87.562	0.084	0.528	368.906	2.072
7	119.992	0.084	0.504	419.944	1.557
8	101.709	0.084	0.510	390.348	1.845
9	132.502	0.084	0.523	442.870	1.367
10	92.786	0.084	0.515	376.053	1.987
11	95.957	0.084	0.510	380.794	1.934
12	108.978	0.084	0.523	403.830	1.735
13	98.451	0.084	0.511	385.112	1.898
14	113.793	0.084	0.510	410.304	1.656
15	102.682	0.084	0.515	392.516	1.831
16	124.773	0.084	0.504	427.911	1.483
17	111.288	0.084	0.511	406.308	1.695
18	135.219	0.084	0.515	446.555	1.326

The Pareto front for temperature and surface roughness for hardness 43 HRC is shown in Figure 5. As shown in Figure 5, the Pareto front consists of 18 pareto-optimal solutions and converged at generation 332. When the cutting parameters are 80.133 m/min, 0.073 mm/rev, and 0.501 mm for cutting speed, feed rate, and depth of cut, the lowest temperature rise achievable using this method is 397.393 °C. Meanwhile, the least surface roughness determined is 0.781 µm, and Table 4 provides the Pareto front solutions.

Because the performance measurements are inherently contradictory, the surface quality degrades as the temperature rises, and the same pattern of performance measures can be seen in the solutions produced for all hardness, as illustrated in Figures 3, 4, and 5 [27]. It also observed that as the hardness of the workpiece is increasing, the temperature rise obtained is increasing but the surface roughness is decreasing. Because none of the Pareto optimum set's solutions is superior to the others, each of them is a viable option. The process engineer's requirements determine if one solution is better than the other. It should be highlighted that all of the solutions are equally good, and depending on the manufacturer's requirements, any set of input parameters can be used to get the matching response values.

The creation of the Pareto-optimal front, which comprises the final set of solutions, is seen in Figures 3, 4, and 5. The continuous nature of the optimization issue addressed determines the form of the Pareto optimum front. The findings in Tables 2, 3, and 4 indicate that the whole range of input parameters is mirrored in 18 Pareto-optimal solutions, with no bias towards the higher or lower side of the parameters. Because the performance measurements are inherently contradictory, the surface quality degrades as the temperature rises, and the same pattern of performance measures is found in the solutions derived for all hardness. As none of the Pareto optimum set's solutions is superior to the others, each of them is a feasible option. The process engineer needs to determine which solution to select. It should be emphasized that all of the solutions are equally effective, and depending on the manufacturer's criteria, any set of input parameters can be used to produce the associated response values.

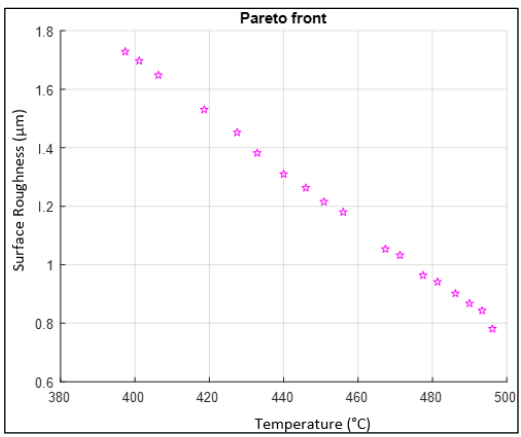

Figure 5: Pareto optimal front for hardness 43 HRC

Effect of cutting speed on the temperature rise and surface roughness

Figure 6 and Table 5 show the interaction effect between cutting speed (*V*) and temperature (*T*) for every hardness. Cutting speed has a considerable impact on temperature rise, as seen in Figure 6. In general, the temperature increase as the cutting speed increase. When the cutting speed is 80 mm/min, the temperature is 243.333 °C, and the temperature increase to 339.731 °C when the cutting speed is 137.579 m/min for hardness 20 HRC. For hardness 36 HRC, the lowest temperature is 363.071 °C for the cutting speed of 85.203 m/min while the highest temperature is 453.044 °C for the cutting speed of 139.969 mm/min. For hardness 43 HRC, the value of cutting speed is 80.133 m/min, the temperature is 397.393 °C. These results are tallying

with the theory of machining. All of the energy lost during the cutting process as a result of plastic deformation is converted to heat, raising the temperature in the cutting zone. Heat generation is inextricably tied to plastic deformation and friction. As the cutting speed rises, friction increases, resulting in a rise in cutting zone temperature [28].

Table 4: Pareto optimal solutions for hardness 43 HRC

No	Cutting speed (mm/min)	Feed rate (mm/rev)	Depth of cut (mm)	Temperature (°C)	Surface roughness (µm)
1	124.587	0.072	0.503	471.252	1.032
2	101.724	0.072	0.500	432.880	1.382
3	109.526	0.072	0.501	445.942	1.263
4	92.886	0.073	0.502	418.628	1.530
5	130.332	0.072	0.508	481.346	0.941
6	128.589	0.072	0.500	477.461	0.964
7	115.327	0.073	0.503	455.988	1.180
8	106.088	0.071	0.500	439.985	1.310
9	137.684	0.074	0.502	493.335	0.843
10	135.799	0.074	0.501	489.958	0.868
11	85.418	0.073	0.502	406.282	1.648
12	133.469	0.073	0.502	486.159	0.902
13	122.544	0.071	0.501	467.345	1.054
14	82.278	0.073	0.502	401.140	1.697
15	112.513	0.072	0.500	450.810	1.215
16	97.936	0.073	0.506	427.472	1.452
17	80.133	0.073	0.501	397.393	1.728
18	139.943	0.071	0.500	496.126	0.781

Table 5: Optimize process predicted by GA

Hardness 20 HRC		Hardness 36 HRC		Hardness 43 HRC	
V (m/min)	*T* (°C)	*V* (m/min)	*T* (°C)	*V* (m/min)	*T* (°C)
80.000	243.333	85.203	363.071	80.133	397.39
89.028	259.079	87.562	368.906	82.278	401.14
106.522	288.388	111.288	406.308	109.526	445.94
111.625	296.957	113.793	410.304	112.513	450.81
135.026	335.284	132.502	442.870	137.684	493.33
137.579	339.731	139.969	453.044	139.943	496.12

The results of the interaction between cutting speed (*V*) and surface roughness (*SR*) are shown in Figure 7 and Table 6. It is obvious that raising the cutting speed reduces surface roughness. This can be proven through

hardness 20 HRC, the surface roughness is 2.867 µm when the cutting speed is 80 m/min and the value of roughness decrease to 1.975 µm when the cutting speed value is 137.579 m/min. This phenomenon occurs for hardness 36 HRC, when the cutting speed value is 85.203 m/min, the surface roughness is 2.103 µm. However, when the value of cutting speed is 139.969 m/min, the value of surface roughness becomes 1.246 µm. The situation also happened for hardness 43 HRC, the value of cutting speed is 80.133 m/min, and the surface roughness value is 2.103 µm. Meanwhile, when the cutting speed value is 139.943 m/min, the value of surface roughness is 0.781 µm. This characteristic is related to the smaller built-up edge size at higher speeds when the built-up edge's impact becomes minimal. Furthermore, when the cutting speed increases, the cutting process becomes steadier, and vibration while cutting at the greatest speed is reduced. The result of the study is consistent with the study made by Anil et al. [29].

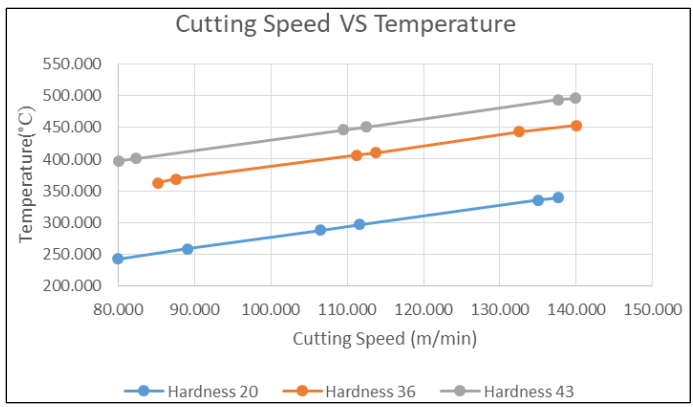

Figure 6: Interaction effect between cutting speed and temperature

Table 6: Optimize process by GA

Hardness 20		Hardness 36		Hardness 43	
V (m/min)	*SR* (µm)	*V* (m/min)	*SR* (µm)	*V* (m/min)	*SR* (µm)
80.000	2.867	85.203	2.103	80.133	1.728
89.028	2.734	87.562	2.072	82.278	1.697
106.522	2.463	111.288	1.695	109.526	1.263
111.625	2.381	113.793	1.656	112.513	1.215
135.026	2.011	132.502	1.367	137.684	0.843
137.579	1.975	139.969	1.246	139.943	0.781

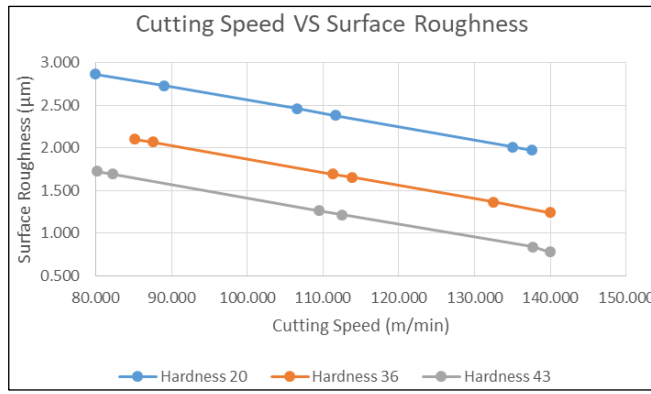

Figure 7: Interaction effect between cutting speed and surface roughness

Effect of feed rate on the temperature rise and surface roughness

Figure 8 depicts the interaction effect between feed rate and temperature for hardness 20 HRC, 36 HRC, and 43 HRC. According to Table 7, increasing the feed rate (*f*) will correspondingly raise the temperature (*T*) during machining. The lowest temperature is 243.333 °C when the feed rate is 0.071 mm/rev. After that, the maximum temperature is 339. 731°C, when the value of the feed rate is 0.072 mm/rev for the hardness 20 HRC. For hardness 36 HRC, the temperature is between 363.071 °C to 453.044 °C even though the feed rate is static at the value 0.084 mm/rev. When the hardness increases to 43 HRC, there are little variations in terms of the value of feed rate. The lowest temperature is 397.393 °C when the feed rate is 0.073 mm/rev and the maximum temperature is 493.335 °C when the feed rate is 0.074 mm/rev. The reason for this is because when the feed rate increases, the contact length between the tool and the workpiece likewise expands. When the feed rate goes up, the chip area rises, which increases the friction between the tool and chip interface, causing the temperature at the tool-chip interface to rise accordingly as well. The results have supported the study that was made by Sulaiman et al. [30], the heat is generated more in the shear zone when the feed rate increases due to the increment in the chip's segment which also contributes to the increase in friction.

The interaction impact between feed rate and surface roughness is depicted in Figure 9 and Table 8. It is seen that a decrease in the feed rate at any setting of cutting speed decreases the surface roughness significantly. This can be seen through the hardness 20 HRC when the feed rate is 0.073 mm/rev. The value of surface roughness is 2.577 µm. For hardness 43 HRC, the value of surface roughness becomes 1.728 µm when the value of the feed rate is 0.073 mm/rev, and the value of surface roughness decreases to 0.781

µm when the feed rate to 0.071 mm/rev. Decreasing feed results in flank wear which will deteriorate the surface of the workpiece.

Table 7: Optimize process by GA

Hardness 20 HRC		Hardness 36 HRC		Hardness 43 HRC	
f (mm/rev)	*T* (°C)	*f* (mm/rev)	*T* (°C)	*f* (mm/rev)	*T* (°C)
0.071	243.33	0.084	363.07	0.073	397.39
0.072	259.07	0.084	368.90	0.073	401.14
0.072	288.38	0.084	406.30	0.072	445.94
0.072	296.95	0.084	410.30	0.072	450.81
0.071	335.28	0.084	442.87	0.072	477.46
0.072	339.73	0.084	453.04	0.074	493.33

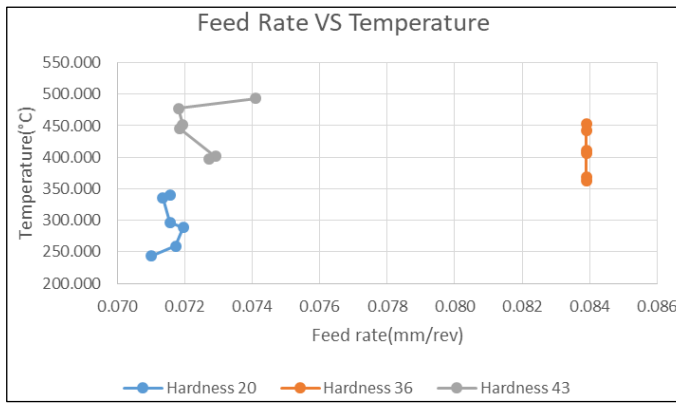

Figure 8: Interaction effect between feed rate and temperature

Table 8: Optimize process by GA

Hardness 20 HRC		Hardness 36 HRC		Hardness 43 HRC	
f (mm/rev)	*SR* (µm)	*f* (mm/rev)	*SR* (µm)	*f* (mm/rev)	*SR* (µm)
0.073	2.577	0.084	2.103	0.073	1.728
0.072	2.463	0.084	2.072	0.073	1.648
0.072	2.381	0.084	1.695	0.073	1.530
0.072	2.294	0.084	1.656	0.072	1.382
0.071	2.113	0.084	1.367	0.072	1.215
0.071	2.055	0.084	1.246	0.071	0.781

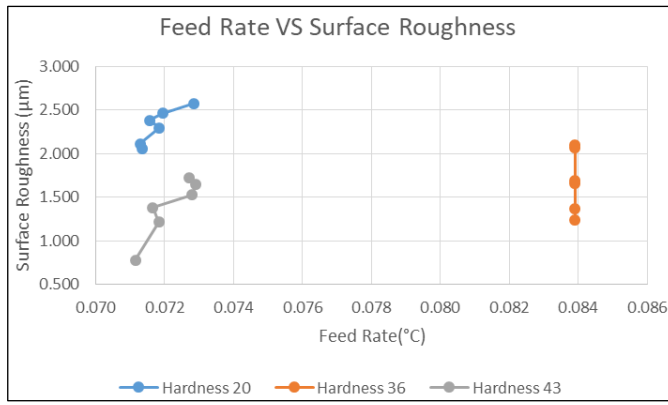

Figure 9: Interaction effect between feed rate and surface roughness

Effect of depth of cut on temperature and surface roughness

Table 9 and Figure 10 indicate the influence of cut depth on temperature. From Figure 10, it can easily find that increasing in the depth of cut (*doc*) will rise the temperature (*T*). It can be seen through the hardness 20 HRC when the temperature is 243.333 °C and the cut depth is 0.5 mm. When the depth of the cut is 0.509 mm, the temperature rises to 325.175 °C. The same thing happened to hardness 36 HRC when the temperature was 427.911 °C and the cut depth was 0.504 mm. However, the temperature rose to 368.906 °C when the depth of cut began to rise by 0.528 mm. The same thing occurred for hardness 43 HRC; at 0.501 mm of cut depth, the temperature was 397.393 °C, and at 0.508 mm of cut depth, the temperature was 481.346 °C. It is possible to argue that as cut depth increases the cutting insert experiences more cutting resistance, which raises temperature. Additionally, the total amount that the cutting tool took from the workpiece's radius during the cutting process was counted. High material hardness demands a deeper value of cut, increasing the strain on the tool and shortening tool life as a result of increased surface roughness.

Table 9: Optimize process by GA

Hardness 20 HRC		Hardness 36 HRC		Hardness 43 HRC	
doc (mm)	*T* (°C)	*doc* (mm)	*T* (°C)	*doc* (mm)	*T* (°C)
0.500	243.333	0.504	427.911	0.501	397.393
0.504	283.728	0.510	410.304	0.502	401.140
0.505	263.391	0.512	424.234	0.503	455.988
0.507	288.388	0.515	446.555	0.503	471.252
0.509	318.181	0.523	442.870	0.506	427.472
0.509	325.175	0.528	368.906	0.508	481.346

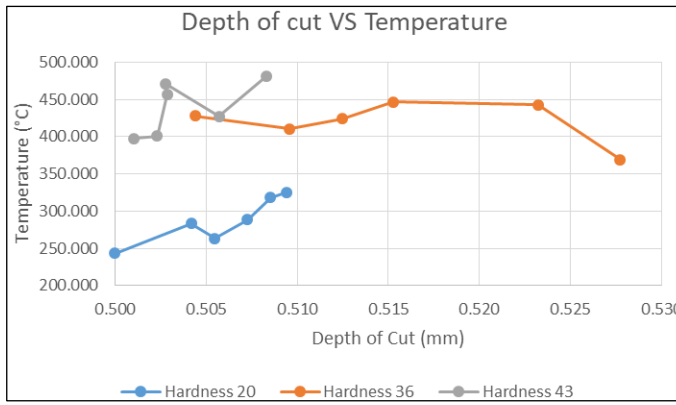

Figure 10: Interaction effect between depth cut and temperature

Table 10 and Figure 11 both display the interaction between surface roughness and depth of cut. It depicts how a deeper cut yields a lower-quality surface. According to Table 10, as the value of the depth of cut increases, so does the value of the surface roughness. With a hardness of 20 HRC, when the depth of cut is 0.502 mm, the surface roughness is 2.055 µm, and when the depth of cut is increased to 0.507 mm, the surface roughness increases to 2.463 µm. For a cut depth of 0.504 mm, the lowest value of surface roughness for hardness 36 HRC is 1.246 µm. The value of surface roughness increases to 2.072 µm when the depth of cut is increased to 0.528 mm. When the surface roughness value is 0.964 µm and the depth of cut value is 0.5 mm, this behaviour occurs for hardness 43. However, the measure of surface roughness increases to 0.941 µm when the depth of cut exceeds 0.508 mm. The cut depth is inversely related to the shear angle and heat-affected zone (HAZ). As the depth of the cut rises, the HAZ and shear angle increase, increasing the cutting force and friction, raising the temperature, and causing the removal of material to deposit on the tool's rake face [29]. As a result, as the depth of the cut rises, the surface roughness (SR) increases as well.

Table 10: Optimize process by GA

Hardness 20		Hardness 36		Hardness 43	
doc (mm)	*SR* (µm)	*doc* (mm)	SR (µm)	*doc* (mm)	SR (µm)
0.502	2.055	0.504	1.246	0.500	0.964
0.502	2.236	0.515	1.326	0.502	0.843
0.504	2.501	0.510	1.656	0.503	1.032
0.505	2.692	0.515	1.987	0.503	1.180
0.505	2.734	0.523	1.735	0.506	1.452
0.507	2.463	0.528	2.072	0.508	0.941

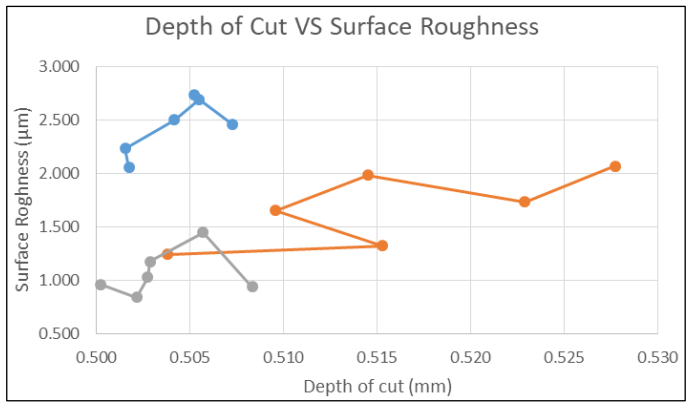

Figure 11: Interaction effect between depth of cut and surface roughness

Effect of the workpiece hardness on the temperature rise and surface roughness

In this study, the effects of workpiece hardness on temperature rise and surface roughness are examined. Changes in the workpiece's surface hardness and roughness measurements were measured throughout the turning process. The three types of workpiece hardness that were used in this study are 20 HRC, 36 HRC, and 43 HRC. It was discovered that surface roughness decreases with increasing hardness, but temperature increases as hardness increases. Table 11 demonstrates that rising temperatures are correlated with increasing levels of hardness. The temperature is between 243 °C and 339 °C, according to hardness 20. When the workpiece's hardness reaches 36, the temperature begins to rise between 363 °C and 453 °C. When the hardness is 43, the value begins to rise, which is between 397 °C and 496 °C. When the hardness is 20 HRC, the value for surface roughness ranges from 2.867 µm to 1.975 µm. When the hardness is 36 HRC, the range starts to widen from 2.103 µm to 1.246 µm. Surface roughness starts to decrease with a hardness of 43 HRC, going from 1.728 µm to 0.781 µm.

According to the table, surface roughness increases in value as material hardness increases. The range of 2.867 µm to 1.975 µm is the surface roughness value for hardness 20 HRC. Surface roughness drops from a value of 2.103 µm to 1.246 µm when hardness rises to 36 HRC. When the hardness is 43 HRC, the surface roughness measurement falls between 1.728 µm and 0.781 µm. Cutting speed significantly affects responses, as seen in Table 11. Lower cutting rates cause a rapid increase in surface roughness, whereas higher cutting speeds cause a quicker increase in hardness. The cutting parameter shows that the independent variable with the greatest influence on the response to the overall turning parameters was cutting

speed, followed by feed rate and depth of cut, which had negligible influence. This study coincides with the study conducted by Omat et al. [31]. As a result, machining has an obvious impact on the workpiece's surface layer's hardness and roughness, both of which are caused by the cutting parameters, particularly cutting speed. The turning process uses cutting force that causes the chips to rip as the tool moves forward, significantly deforming the plastic at the surface and in the layer's underneath. This deformation aftereffect will affect the metal ductility, hardness, and strength. Meanwhile, the underlying material fracture occurs as a result of the chip's severe deformation, resulting in poor surface roughness. The metal characteristics are also affected by the form, size, and depth of cut of the surface grooves.

The ability of a solid substance to endure persistent deformation without shattering is known as ductility in materials science. Ductility is also known as fracture strain or percent reduction in area. Increased surface hardness of the specimens resulted in a decrease in fracture strain. As a result of the plastic deformation created during machining, the material was projected to have been extended over a portion of its permitted plastic deformation, and hence the ductility of the hardened workpieces should have been reduced. Cutting speed had a significant impact on ductility, with high speeds resulting in a higher fracture strain value. This is because the surface roughness rises as the cutting speed lowers [32].

Table 11: Temperature range for every hardness

Hardness (HRC)	Cutting speed (m/min)	Feed rate (mm/rev)	Depth of cut (mm)	Temperature (°C)	Surface roughness (µm)
20	80 -	0.073 -	0.502 -	243 - 339	2.867 -
36	85.203 -	0.084	0.504 -	363 - 453	2.103 -
43	80.133 -	0.073 -	0.5 -	397 - 496	1.728 -

Conclusion

The study showed how to use MOGA to optimize the turning process. The findings suggest that MOGA can yield optimal process parameters and may be used to successfully optimize turning, demonstrating that MOGA is a beneficial optimization tool. The following conclusions may be taken from the optimization conducted on the turning machining process using MOGA:

i. Due to the contradiction between surface roughness and temperature rise and the machining output, MOGA was able to determine a trade-off between these two objective functions by identifying a combination

of feed rate, cutting speed, and depth of cut that satisfied both objective functions.

ii. According to the results, the feed rate, cutting speed, and depth of cut are all significant causes of temperature rise and surface roughness.

iii. As the cutting speed increases, surface roughness decreases while the temperature rises.

iv. The temperature is improved by raising the feed rate, while surface roughness is greatly reduced when the feed rate is increased at any cutting speed.

v. The temperature is going to increase as the depth of the cut increases, and the surface roughness value will begin to rise as well.

vi. Although the surface roughness decreases as the hardness increases, the temperature rises as the hardness increases.

vii. When the cutting parameters are 80 m/min, 0.071 mm/rev, and 0.5 mm for cutting speed, feed rate, and depth of cut for hardness 20 HRC, the lowest temperature rise that can be achieved using this method is 243.333 °C. Accordingly, it was found that employing MOGA to optimize the machining settings for 20 HRC has improved the temperature rise by about 10.2% and surface roughness by about 20%.

viii. Meanwhile, when the cutting speed, feed rate, and depth of cut lowest surface roughness measured for hardness 36 HRC was 1.246 µm. The values are 85.023 m/min, 0.084 mm/rev, and 0.504 mm, respectively. 363.071 °C is the lowest temperature rise that can be produced using these combined parameters. Both temperature rise and surface roughness have increased by 34% as a result of the optimization for 36 HRC.

ix. The lowest temperature rise possible with this method is 397.393 °C when the cutting parameters are 80.133 m/min, 0.073 mm/rev, and 0.501 mm for cutting speed, feed rate, and depth of cut with hardness 43 HRC. The lowest surface roughness that has been identified is 0.781 µm. By optimizing the machining parameters for 43HRC, the temperature increase has improved by 34% and the surface roughness has improved by 4%.

Contributions of Authors

The authors confirm the equal contribution in each part of this work. All authors reviewed and approved the final version of this work.

Funding

This work was supported by the "UMP Fundamental Research Grant" [RDU1803144, Optimization of Machining Parameters on Temperature Rise In Cnc Turning of Al 6063 Using Genetic Algorithm, 2018].

Conflict of Interests

All authors declare that they have no conflicts of interest.

Acknowledgement

The authors acknowledge the UMP Fundamental Research Grant (RDU1803144) from Universiti Malaysia Pahang for providing financial support, and also for the use of the research facilities through the course of this research

References

[1] A. F. Zubair and M. S. Abu Mansor, "Embedding firefly algorithm in optimization of CAPP turning machining parameters for cutting tool selections," *Computer & Industrial Engineering*, vol. 135, pp. 317–325, 2019. doi: 10.1016/j.cie.2019.06.006.

[2] B. N. K. P. P. Shirpurkar, S.R. Bobde, V.V.Patil, "Optimization of Turning Process Parameters by Using Tool Inserts- A Review," *International Journal of Engineering and Innovative Technology (IJEIT)*, vol. 2, no. 6, pp. 216–223. 2012.

[3] L. B. Abhang and M. Hameedullah, "Optimization of machining parameters in steel turning operation by Taguchi method," *Procedia Engineering*, vol. 38, pp. 40–48, 2012. doi: 10.1016/j.proeng.2012.06.007.

[4] M. Gopal, "Optimization of machining parameters on temperature rise in CNC turning process of aluminium 6061 using rsm and genetic algorithm," *International Journal of Modern Manufacturing Technologies*, vol. 12, no. 1, pp. 36–43, 2020.

[5] C. S. Akhil, M. H. Ananthavishnu, C. K. Akhil, P. M. Afeez, R. Akhilesh, and R. Rajan, "Measurement of Cutting Temperature during Machining," *Journal of Mechanical and Civil Engineering*, vol. 13, no. 2, pp. 102–116, 2016. doi: 10.9790/1684-130201102116.

[6] M. Kuntoğlu, A. Aslan, H. Sağlam, D. Y. Pimenov, K. Giasin, and T. Mikolajczyk, "Optimization and analysis of surface roughness, flank wear and 5 different sensorial data via tool condition monitoring system in turning of aisi 5140," *Sensors (Switzerland)*, vol. 20, no. 16, pp. 1–22, 2020. doi: 10.3390/s20164377.

[7] D. Y. Pimenov, A. Bustillo, S. Wojciechowski, V. S. Sharma, M. K. Gupta, and M. Kuntoğlu, "Artificial intelligence systems for tool condition monitoring in machining: analysis and critical review," *Journal of Intelligent Manufacturing*, vol. 34, pp. 2079-2121, 2023, doi: 10.1007/s10845-022-01923-2.

[8] N. Amulya, P. V. S. Subhashini, K. Chinmayi, and R. Naveen, "Parametric Optimization of Heat Generation during Turning Operation," *Journal of Mechanical Engineering and Automation*, vol. 6, no. 5A, pp. 117–120, 2016. doi: 10.5923/c.jmea.201601.22.

[9] N. H. A. Halim, C. H. C. Haron, J. A. Ghani, and M. F. Azhar, "Prediction of cutting force for milling of Inconel 718 under cryogenic condition by response surface methodology," *Journal of Mechanical Engineering*, vol. 16, no. 1, pp. 1–16, 2019.

[10] T. H. Bhuiyan and I. Ahmed, "Optimization of Cutting Parameters in Turning Process," *SAE International Journal of Materials and Manufacturing*, vol. 7, no. 1, pp. 233–239, 2014. doi: 10.4271/2014-01-9097.

[11] A. Debroy and S. Chakraborty, "Non-conventional optimization techniques in optimizing non-traditional machining processes: A review," *Management Science Letters*, vol. 4, no. 1, pp. 23–38, 2013. doi: 10.5267/j.msl.2012.10.038.

[12] H. Akkus and H. Yaka, "Optimization of Turning Process by Using Taguchi Method," *Sakarya University Journal of Science*, vol. 22, no. 5, pp. 1–1, 2018. doi: 10.16984/saufenbilder.409502.

[13] S. Krishna Madhavi, D. Sreeramulu, and M. Venkatesh, "Evaluation of Optimum Turning Process of Process Parameters Using DOE and PCA Taguchi Method," *Materials Today Proceedings*, vol. 4, no. 2, pp. 1937–1946, 2017. doi: 10.1016/j.matpr.2017.02.039.

[14] T. S. S.P. Palaniappan, K. Muthukumar, R.V. Sabariraj , S. Dinesh Kumar, "CNC turning process parameters optimization on Aluminium 6082 alloy by using Taguchi and ANOVA," *Materials Today Proceedings*, vol. 20, pp. 342–347, 2020. doi: 10.1016/j.matpr.2019.10.053.

[15] D. R. Shah, N. Pancholi, H. Gajera, and B. Patel, "Investigation of cutting temperature, cutting force and surface roughness using multi-objective optimization for turning of Ti-6Al-4 V (ELI)," *Materials Today: Proceedings*, vol. 50 no. 5, pp. 1379-1388, 2021. doi: 10.1016/j.matpr.2021.08.285.

[16] O. Manav and S. Chinchanikar, "Multi-Objective Optimization of Hard Turning: A Genetic Algorithm Approach," *Materials Today Proceedings*, vol. 5, no. 5, pp. 12240–12248, 2018. doi: 10.1016/j.matpr.2018.02.201.

[17] V. Durga Prasad Rao, S. R. S. Mahaboob Ali, S. M. Z. M. Saqheed Ali, and V. Navya Geethika, "Multi-objective optimization of cutting parameters in CNC turning of stainless steel 304 with TiAlN nano coated tool," *Materials Today Proceedings*, vol. 5, no. 12, pp. 25789–25797, 2018. doi: 10.1016/j.matpr.2018.06.571.

[18] N. Sathiya Narayanan, N. Baskar, and M. Ganesan, "Multi Objective Optimization of machining parameters for Hard Turning OHNS/AISI H13 material, Using Genetic Algorithm," *Materials Today: Proceedings*, vol. 5, no. 2, pp. 6897–6905, 2018. doi: 10.1016/j.matpr.2017.11.351.

[19] A. Kumar, S. K. Pradhan, and V. Jain, "Experimental investigation and optimization using regression genetic algorithm of hard turning operation with wiper geometry inserts," *Materials Today: Proceedings*, vol. 27, pp. 2724–2730, 2019. doi: 10.1016/j.matpr.2019.12.191.

[20] R. Butola, S. Kanwar, L. Tyagi, R. M. Singari, and M. Tyagi, "Optimizing the machining variables in CNC turning of aluminum based hybrid metal matrix composites," *SN Applied Sciences*, vol. 2, no. 8, pp. 1–9, 2020. doi: 10.1007/s42452-020-3155-8.

[21] M. Mia and N. R. Dhar, "Modeling of Surface Roughness Using RSM, FL and SA in Dry Hard Turning," *Arabian Journal for Science and Engineering*, vol. 43, no. 3, pp. 1125–1136, 2018. doi: 10.1007/s13369-017-2754-1.

[22] Y. Ren, S. Rubaiee, A. Ahmed, A. M. Othman, and S. K. Arora, "Multi - objective optimization design of steel structure building energy consumption simulation based on genetic algorithm," *Nonlinear Engineering*, vol. 11, no. 1, pp. 20–28, 2022. doi: 10.1515/nleng-2022-0012.

[23] A. Chabbi, M. A. Yallese, M. Nouioua, I. Meddour, T. Mabrouki, and F. Girardin, "Modeling and optimization of turning process parameters during the cutting of polymer (POM C) based on RSM, ANN, and DF methods," *International Journal of Advanced Manufacturing Technology*, vol. 91, no. 5–8, pp. 2267–2290, 2017. doi: 10.1007/s00170-016-9858-8.

[24] B. Solarte-Pardo, D. Hidalgo, and S. S. Yeh, "Cutting insert and parameter optimization for turning based on artificial neural networks and a genetic algorithm," *Applied Sciences (Switzerland)*, vol. 9, no. 3, 2019. doi: 10.3390/app9030479.

[25] S. H. Yang and U. Natarajan, "Multi-objective optimization of cutting parameters in turning process using differential evolution and non-

dominated sorting genetic algorithm-II approaches," *International Journal of Advanced Manufacturing Technology*, vol. 49, no. 5–8, pp. 773–784, 2010. doi: 10.1007/s00170-009-2404-1.

[26] D. Tanikić, "Computationally intelligent optimization of metal cutting regimes," *Measurement*, vol. 152, p. 107358, 2020. doi: 10.1016/j.measurement.2019.107358.

[27] E. G. Ng, D. K. Aspinwall, D. Brazil, and J. Monaghan, "Modelling of temperature and forces when orthogonally machining hardened steel," *International Journal of Machine Tools and Manufacture*, vol. 39, no. 6, pp. 885–903, 1999. doi: 10.1016/S0890-6955(98)00077-7.

[28] S. Sivarajan and R. Padmanabhan, "Green machining and forming by the use of surface coated tools," *Procedia Engineering*, vol. 97, pp. 15–21, 2014. doi: 10.1016/j.proeng.2014.12.219.

[29] K. C. Anil, M. G. Vikas, B. Shanmukha Teja, and K. V. Sreenivas Rao, "Effect of cutting parameters on surface finish and machinability of graphite reinforced Al-8011 matrix composite," *IOP Conference Series: Materials Science and Engineering*, vol. 191, no. 1, pp. 1-5, 2017. doi: 10.1088/1757-899X/191/1/012025.

[30] S. Sulaiman, A. Roshan, and S. Borazjani, "Effect of cutting parameters on cutting temperature of TiAL6V4 alloy," *Applied Mechanics and Materials*, vol. 392, no. September, pp. 68–72, 2013. doi: 10.4028/www.scientific.net/AMM.392.68.

[31] O. J. Zurita-Hurtado, V. C. Di Graci-Tiralongo, and M. C. Capace-Aguirre, "Effect of surface hardness and roughness produced by turning on the torsion mechanical properties of annealed AISI 1020 steel," *Revista Facultad de Ingenieria*, vol. 2017, no. 84, pp. 55–59, 2017. doi: 10.17533/udea.redin.n84a07.

[32] H. Sasahara, "The effect on fatigue life of residual stress and surface hardness resulting from different cutting conditions of 0.45%C steel," *International Journal of Machine Tools and Manufacture*, vol. 45, no. 2, pp. 131–136, 2005. doi: 10.1016/j.ijmachtools.2004.08.002.